Generalized model of island biodiversity

David A. Kessler and Nadav M. Shnerb
Department of Physics, Bar-Ilan University, Ramat-Gan IL52900, Israel
(Received 18 August 2014; published 10 April 2015)

The dynamics of a local community of competing species with weak immigration from a static regional pool is studied. Implementing the generalized competitive Lotka-Volterra model with demographic noise, a rich dynamics with four qualitatively distinct phases is unfolded. When the overall interspecies competition is weak, the island species recapitulate the mainland species. For higher values of the competition parameter, the system still admits an equilibrium community, but now some of the mainland species are absent on the island. Further increase in competition leads to an intermittent "disordered" phase, where the dynamics is controlled by invadable combinations of species and the turnover rate is governed by the migration. Finally, the strong competition phase is glasslike, dominated by uninvadable states and noise-induced transitions. Our model contains, as a special case, the celebrated neutral island theories of Wilson-MacArthur and Hubbell. Moreover, we show that slight deviations from perfect neutrality may lead to each of the phases, as the Hubbell point appears to be quadracritical.

DOI: 10.1103/PhysRevE.91.042705 PACS number(s): 87.23.Cc, 87.10.Mn, 64.60.Ht, 05.40.Ca

I. INTRODUCTION

Trying to characterize and quantify the factors that govern the dynamics of natural populations, community ecologists were often surprised by the large number of competing species that can be found in a relatively small area. Having in mind the Darwinian picture of natural selection and the survival of the fittest, one may expect that a few fittest species will dominate the community (perhaps with some sporadic presence of a few individuals of inferior species) as suggested by the competitive exclusion principle [1]. This is definitely not the case in many important communities, from tropical forests to coral reef to freshwater plankton. In fact, an understanding of the factors that allow the maintenance of biodiversity under selective dynamics is considered as one of the most important challenges for modern science [2].

One of the versions of the biodiversity puzzle has to do with a local community which is coupled by migration to a regional pool. The simplest example of this scenario is the mainland-island system, where the mainland dynamics is assumed to be relatively slow so one can assume that the island is interacting with (i.e., receiving immigration from) a static pool on the mainland. This mainland-island model may describe any local community, provided that the length scale involved in biological interactions (e.g., competition) is much smaller than the migration scale [3].

In general, the dynamics of natural ecological communities is subject to substantial noise. Populations are exposed to environmental variations that affect their reproductive ability and death rate. This effect is, typically, quite strong [4,5]. Even under strictly fixed environmental conditions, the stochasticity of the birth-death-migration process (demographic stochasticity) adds randomness to the dynamics. Under demographic noise, every finite population goes extinct eventually, so theories of community dynamics must include a stabilizing mechanism that makes these extinctions extremely rare (stable coexistence) or allow for either immigration or a speciation process to maintain the species richness (unstable coexistence) [6].

In the mainland-island system the role of noise is more subtle. On the one hand, in a local community there are at least a few extinction-prone low-abundance species. On the other hand, there are no absorbing states in the strict sense, as individuals of any species arrive at a fixed average rate from the mainland. Nevertheless, if the migration is relatively weak and the local population is not huge, some or perhaps all of the species may undergo temporary extinctions, leaving the island without individuals of this species until an immigrant arrives from the mainland and manages to reestablish the species. The statistics of these local extinction-recolonization events for birds in North America was recently analyzed by Bertuzzo *et al.* [7]. In the discussion section, we will consider the relation between our model and these empirical results.

Community dynamics theories are usually classified along the line between niche and neutral. A niche theory assumes that every species that has a nonsporadic presence on the island has its own niche. For example, a few bird species each having a different beak size and (correspondingly) different diet may coexist on the island if the overlap between the niches is not too large. At the other extreme, a perfectly neutral dynamics admits no niche partitioning at all, with all species using the same resources with the same efficiency, and the dynamics governed solely by stochasticity. In-between, one can find a few "continuum models" [8–11] that were suggested in the last decade and incorporate elements of neutral dynamics with (usually weak) selective effects.

The simplest model for island dynamics is the generalized competitive Lotka-Volterra model (GCLV) with migration. This model is widely used in ecology and for other applications [12–14]. Our primary focus is on an individual based stochastic version of the model which incorporates demographic noise. We will see that the model, despite its simplicity, is very rich and exhibits a wide range of different behaviors. Our goal here is to exhibit this panoply of "phases" and understand their origins. A parallel study of the much more tractable deterministic version of the model will be a key tool in unraveling the dynamics.

Moreover, we shall show in the following that the most celebrated models of island biogeography, the Wilson-MacArthur theory of island biogeography [15,16] and Hubbell's neutral theory of biodiversity [17,18], are two special cases of this model. Following a few recent publications that emphasized some specific aspects of the dynamics [19,20], we would like

to show how the phase structure of the model is governed to a large extent by these two special limits. Finally, we will consider the relevance of this model to the empirical findings.

II. STOCHASTIC GCLV MODEL

In this section, we introduce our model and set notation. Let us consider a regional pool of Q species on the mainland. Each individual of these species may immigrate to the island with a certain probability per unit time, and we denote the average rate at which individuals of the ith species reach the island as λ_i.

Denoting by N_i the abundance of the ith species on the island, the deterministic part of the dynamics satisfies

$$\dot{N}_i = \lambda_i + \alpha_i N_i - \frac{N_i}{K_i}\left(N_i + \sum_{j\neq i} d_{i,j} N_j\right); \quad i = 1,\ldots,Q. \tag{1}$$

Here, α_i is the growth rate of the ith species on the island, and K_i sets the carrying capacity of the ith species. Interspecific interactions are expressed by the elements of the matrix $d_{i,j}$. In this work, we study a purely competitive system where all the $d_{i,j} \geqslant 0$.

As our goal is to identify the different phases of this model, not to fit it to a specific empirical system, we make a few simplifications. First, we assume (as in [21], for example) that all species have the same flux of immigrants from the mainland $\lambda_i = \lambda$, the same linear growth rate that we scale to one ($\alpha_i = 1$), and the same carrying capacity K. We are interested here specifically in small values of λ, so that immigration primarily serves to "rescue" extinct species, but does not swamp the intrinsic competitive dynamics on the island, as discussed in the following. The interaction matrix takes the form $d_{i,j} = Cc_{i,j}$, where C sets the overall strength of the interaction and the set of $c_{i,j}$ is normalized such that

$$\sum_{i\neq j} c_{i,j} = Q(Q-1). \tag{2}$$

In other words, the average magnitude of a $c_{i,j}$ is unity. We consider here the case where the $c_{i,j}$ are chosen randomly from a distribution with unit mean and variance σ^2; the $c_{i,j}$ values are kept fixed throughout the process. The current work considers the case of a purely competitive community without symbiosis or food web features. Accordingly, we do not consider here the case of interaction matrices with a modular or nested structure. As we shall show in the following, this structureless matrix provides a natural generalization of the Hubbell neutral theory [17]. For our simulations, the $c_{i,j}$ were chosen from a gamma distribution with probability distribution function

$$P(c) = \frac{c^{1/\sigma^2-1}\sigma^{-2/\sigma^2}e^{-c/\sigma^2}}{\Gamma(1/\sigma^2)}. \tag{3}$$

The final form of our (deterministic) GCLV model is then

$$\dot{N}_i = \lambda + N_i - \frac{N_i}{K}\left(N_i + C\sum_{j\neq i} c_{i,j} N_j\right). \tag{4}$$

For small immigration rate λ, extinctions and recolonizations play a crucial role in the dynamics. We treat this by constructing a stochastic individual based version of the model, so that demographic noise is explicitly included. The number of individuals in each species is an integer. At each time step of duration Δ, a Poisson number of immigrants of each species, with mean $\lambda\Delta$, is generated. A Poisson number of offspring of each species, with mean $N_i\Delta$, is generated as well. The N_i veteran inhabitants are subject to death, with the number of individuals of species i that expire drawn from a binomial distribution with parameters N_i and probability $\Delta\sum_j(\delta_{i,j} + Cc_{i,j})N_j$. Clearly, Δ needs to be chosen to be sufficiently small that this probability does not exceed unity. The number of individuals of species i after this process is then updated to reflect the new immigrants, offspring, and deaths. On average, these changes are exactly those given by the deterministic model.

The stochastic model is specified by four parameters: K, λ, C, and σ. In what follows, we will focus our attention on the phases in the $\sigma - C$ plane, keeping K and the migration rate fixed. Once this behavior is understood it is straightforward to figure out at least the qualitative features of the dynamics for other values of migration and K. The different phases in the $\sigma - C$ plane are sketched in Fig. 1. In the following, we intend to discuss each phase in detail; before doing that, let us focus on two very interesting limits that correspond to the x and y axes of Fig. 1.

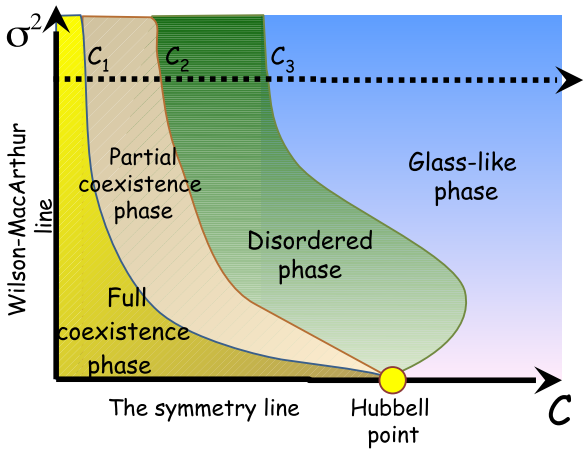

FIG. 1. (Color online) A schematic sketch of the C-σ^2 plane, showing the different phases of the generalized competitive Lotka-Volterra system, as will be discussed following. On the $C = 0$ line there is no competition, all species have the same carrying capacity, and the extinction-recolonization dynamics is described by the Wilson-MacArthur theory. At the Hubbell point, $C = 1$ and $\sigma = 0$, all individuals are equivalent and the system supports a marginally stable manifold on which the dynamics is governed only by the noise. In the weak competition region (small C, labeled "full coexistence phase") all the mainland species are still semiresident on the island, but with heterogeneous abundance and extinction times. Above C_1, some species are transients, with $\mathcal{O}(\lambda)$ abundance ("partial coexistence phase"). Another increase in the strength of competition takes the system to the disordered, intermittent phase, where the community structure changes dramatically over time and the instantaneous assembly is usually invadable. Finally, in the glasslike phase a few uninvadable equilibria control the system and the transitions are noise induced.

III. WILSON-MACARTHUR LINE $C = 0$

When $C = 0$, species do not interact with each other and the dynamics of each species is logistic with carrying capacity K. Deterministically, an infinitesimally small population grows exponentially and then saturates to the steady state value K. With demographic noise, the first immigrant may fail to establish a community (e.g., it may die before reproduction, even if the birth rate is larger than the death rate), so not every immigration results in successful colonization. The chance of a successful colonization depends on the details of the stochastic process (in particular, the variance in the number of offspring per individual, see the analysis of [22] for the mathematically equivalent SIS infection model). After a successful recolonization, the population will again fluctuate around K, and in the long run it must go extinct as well since (without migration) the zero population is an absorbing state. The rate of these long-term extinctions (as opposed to colonization failures that take place at short times) depends, again, on the details of the process and the value of K [23].

Accordingly, in the $C = 0$ limit of our model the history of every species is made of a series of local extinctions and recolonization events, and the rates of extinction and recolonization are equal for all species. What emerges from this scenario is the celebrated Wilson-MacArthur model of island biogeography: the species richness on the island S satisfies $\dot{S} = -eS + r(Q - S)$, where e is the extinction rate and r is the recolonization rate, and both rates depend on K and on the details of the stochastic process. The Wilson-MacArthur prediction for the average species richness is $\bar{S} = rQ/(r + e)$, the typical size of species richness fluctuations is $\sqrt{reQ}/(r + e)$, and the statistics of persistence times [24], the periods between colonization and extinction (as well as the periods between extinction and colonization), is exponential.

When the only stochastic effect taken into account is demographic noise, as is the case in this paper, the chance of extinction decreases exponentially with K [25] and therefore for the typical values of K considered here $e \ll 1$. If this is actually the case, or when λ is large so that $r \to \infty$, all mainland species are present on the mainland except for rare short-term fluctuations and so $S \approx Q$. Accordingly, in our model one observes Wilson-MacArthur dynamics on reasonable time scales only when K is relatively small. More realistic models have to take into account other types of noise (including environmental variations, attacks by pathogens, etc.) that may lead to extinction, and the Wilson-MacArthur model will then be relevant even for higher values of K.

IV. SYMMETRY LINE AND THE HUBBELL POINT

On the x axis, the $\sigma = 0$ line, species do interact with each other but the interaction is symmetric, i.e., no change in community dynamics occurs upon switching the species labels of any given populations. C measures the strength of interspecific competition: if $C < 1$, the intraspecific competition is stronger than the interspecific (reflecting mechanisms such as resource partitioning or frequency dependent predation) and a low-density species may invade the system. On the other hand, for any $C > 1$ the intraspecific competition is weaker than the interspecific, resulting in competitive exclusion [6]. At the boundary between these regimes, one finds the Hubbell point $C = 1$ (see Fig. 1). At the Hubbell point, the model is *neutral*: any individual competes equally with any other individual and the strength of each pair competition is fixed and independent of species affiliation.

Without immigration, the deterministic GCLV supports, to the left of the Hubbell point, an egalitarian coexistence stable fixed point where all species are present on the island with the same abundance $K/[1 + (Q - 1)C]$, while above the Hubbell point the stable solution admits only one species with abundance K, and all other species have zero abundance (the identity of the surviving species is determined by initial conditions). At the Hubbell point, the deterministic dynamics supports a marginal manifold: every combination of N_i's such that the total population is K is a solution of Eq. (4). The simplicity of the GCLV at the Hubbell point allows one to solve analytically for the species abundance distributions (SAD) even with demographic noise [26], environmental stochasticity [27], or a combination of demographic and environmental noise [28].

About 15 years ago, Hubbell [17] put forward his very influential neutral theory of biodiversity, suggesting that all species and all individuals are demographically equivalent and the only mechanism that drives the system is pure demographic noise and the (typically slow) rate at which new species are introduced. Hubbell's model has two versions. In the metacommunity version, speciation is the mechanism that leads to the introduction of a new species, while in the mainland-island version colonizers of new species arrive from the mainland (assuming large Q). Some patterns predicted by this neutral theory, and in particular the species abundance distribution (SAD) on the island, fit quite nicely those recorded in many empirical studies [18,29].

Moving off the Hubbell point but remaining on the x axis, $\sigma = 0$, the infinite degeneracy is lifted, but the analysis of the stochastic system is still relatively easy since every species may be analyzed independently, the effect of all individuals from other species being encapsulated into a single parameter. This feature was exploited in [20] to solve the (metacommunity version) stochastic GCLV analytically along the $\sigma = 0$ line. As expected, below the Hubbell point, the SAD shows a peak around the deterministic value $QK/[1 + (Q - 1)C]$, and the sharpness of this peak increases as C decreases.

V. AN OVERVIEW OF THE DYNAMICS

Having examined the $\sigma = 0$ and $C = 0$ limits, we now turn to the results of the model for general σ, C. We present in Fig. 2 sample runs of the system for $K = 100$, $\lambda = 0.01$, $\sigma = 0.5$, $Q = 20$, for varying C. The abundance of each species is indicated by color. The horizontal axis is time, with snapshots of the system taken every $t = 0.08/\lambda$. The vertical axis is species number, and runs from 1 to $Q = 20$. It is clear that the system exhibits very different behavior as C is varied. One can identify four different generic behaviors, which we shall call "phases." Very briefly, in the first, low C, phase (represented by the first panel in Fig. 2), all Q species are present essentially all the time. In the second (represented by the next two panels), some species are basically no longer present, supported only by the infrequent stochastic immigration of

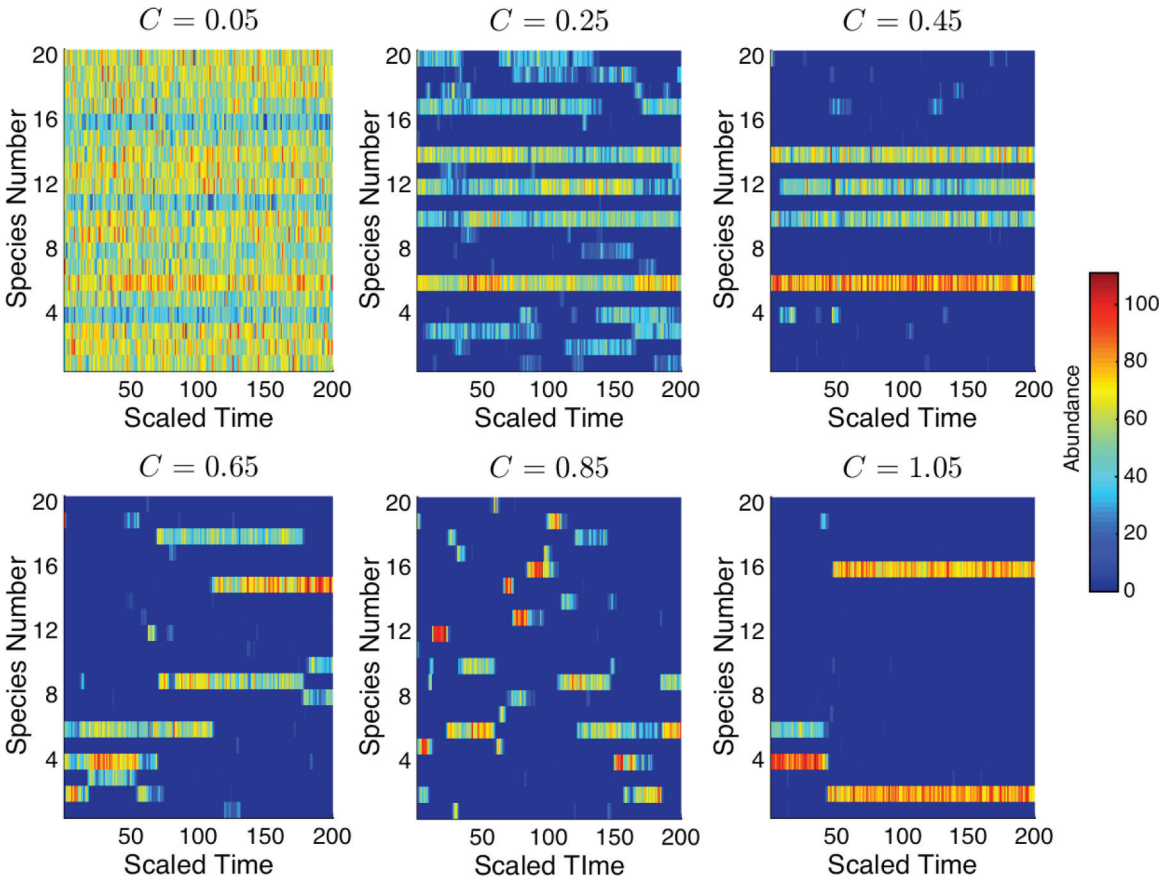

FIG. 2. (Color) Snapshots of the abundance for all species in the stochastic model for various levels of competition C. Red is high abundance, dark blue low, as shown in the color bar at the right. $Q = 20$, $K = 100$, $\sigma = 0.5$, $\lambda = 0.01$. The time is measured in units of $0.08/\lambda$. The first panel exhibits full coexistence, the second and third partial coexistence, the fourth and fifth disorder dynamics, and the last glasslike dynamics.

new individuals, while the rest have a more or less continuous existence, with occasional temporary extinctions. The third phase (represented by the fourth and fifth panels) at yet higher C is the most complicated, with the system jumping from one set of dominant species to a completely different set. These states would be stable in the absence of immigration, but a successful colonization by some specific species drives the system to a new quasistable state. In the last phase (represented by the last panel), the system spends a preponderance of time in some stable state. In the following, we will attempt to explicate in more detail the various features of each of these phases.

One way to quantify the different behaviors is via the "inverse participation ratio" (IPR), defined as

$$\mathrm{IPR} \equiv \frac{\left(\sum_{i=1}^{Q}\langle N_i\rangle\right)^2}{\sum_{i=1}^{Q}\langle N_i\rangle^2}. \tag{5}$$

The angle brackets refer to an average over time. The IPR varies from 1 to Q. In the case where only one species is present, it takes the value unity, and if all species have equal abundance, its value is Q. Thus, the IPR is a measure of how many different species are active in the system altogether. It can differ enormously from the time average of the instantaneous number of species present. We show in Fig. 3 the IPR as a function of C for runs with the same parameters as in Fig. 2. We see that the IPR is not monotonic in C. It initially decreases from Q, reaches a minimum, and then starts to increase. It then achieves a local maximum and then starts to decrease again.

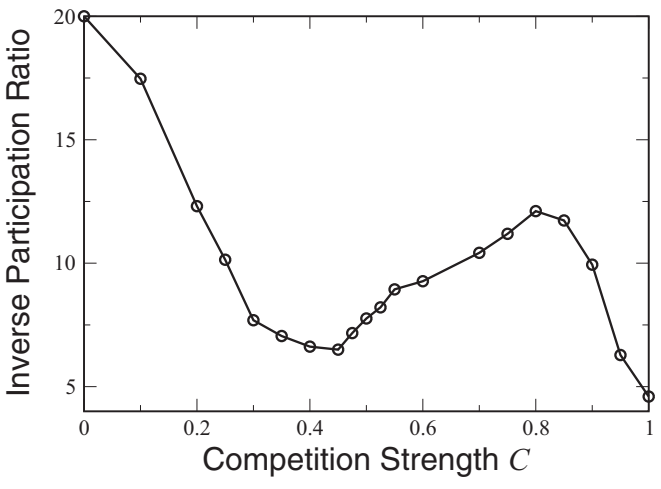

FIG. 3. The inverse participation ration (IPR), as a function of C. $N = 20$, $K = 100$, $\sigma = 0.5$, $\lambda = 0.01$. The onset of Phase III is associated with the beginning of the rise of the IPR at $C \approx 0.47$ and the onset of Phase IV with the beginning of the fall at $C \approx 0.80$.

This change in behavior of the IPR is clearly reflective of the different patterns captured in Fig. 2. We shall elaborate on the behavior of the IPR as we investigate each phase.

VI. PHASE I: THE FULL COEXISTENCE PHASE

We start by considering the leftmost region of Fig. 1, the area where C is relatively small. Increasing C from zero, at a fixed value of σ, corresponds to an increase of interspecific competition; for example, different species of birds that live happily together, each having a different diet of worms, may start to interact with each other if the supply of worms is decreased and different species begin to consume the same resource. In such a case, species-specific niches are "squeezed" towards each other, increasing the niche overlap.

Once the species start to compete, the heterogeneity of the $c_{i,j}$'s (as reflected in the parameter σ) implies that some species are impacted by the competition more than the others. As a result, the abundance N_i of the ith species is no longer K (as on the Wilson-MacArthur line $C = 0$); instead, all abundances are reduced by a species-dependent amount and one gets a distribution of species abundance values. Still, as long as C is not too large, the deterministic dynamics of Eq. (1) supports a single attractive fixed point that corresponds to the case where all the Q species of the mainland are represented on the island. In this case, the effect of migration (λ) is weak since the small external flux does not qualitatively change the steady state, which in any case has all species present. The steady state is then well approximated by the solution of Eq. (1) with $\lambda = 0$, which is easily seen to be

$$N_i = K B^{-1} \mathbb{1}, \tag{6}$$

where $\mathbb{1}$ stands for the length Q column vector consisting of all ones, and B is the matrix

$$B_{i,j} = \delta_{i,j} + C c_{i,j}. \tag{7}$$

Figure 4 illustrates the process. For C small enough that coexistence fixed point solution is physical, such that all N_i are positive, there is a unique stable solution and all Q mainland species will be present on the island. Their respective abundances decrease as a function of C, but no species goes extinct in the deterministic theory. As long as this remains true, for reasonably large K one can more or less neglect the noise, given the stability of the fixed point solution. The species that have lower abundance are those who suffer more from the competition, and even if demographic noise drives a few of them to extinction, the effect on the rest of the network is minor and the system will restore itself by immigration. This situation is illustrated by the first panel of Fig. 2, the case $C = 0.05$, where there are no extinctions seen in the timeframe shown. Examined over a much longer period, there are indeed a few occasional extinctions, followed by recolonization via immigration, of various species. The most extinction prone species, for example, was seen to go extinct a total of four times over a period of 24 000 snapshots. The IPR, initially equal to Q at $C = 0$, will decrease with increasing C, due to the increasing nonuniformity of the various population sizes.

In such a scenario, one expects deviations from the Wilson-MacArthur formula. When the abundance of the species are different from each other, the chance of extinction e becomes species dependent, so once $C > 0$ the persistence times will reflect a convolution of exponents with different time scales. When the community heterogeneity increases, the Wilson-MacArthur extinction-recolonization dynamics is most relevant for the smaller species, again with heterogeneous statistics of extinction times.

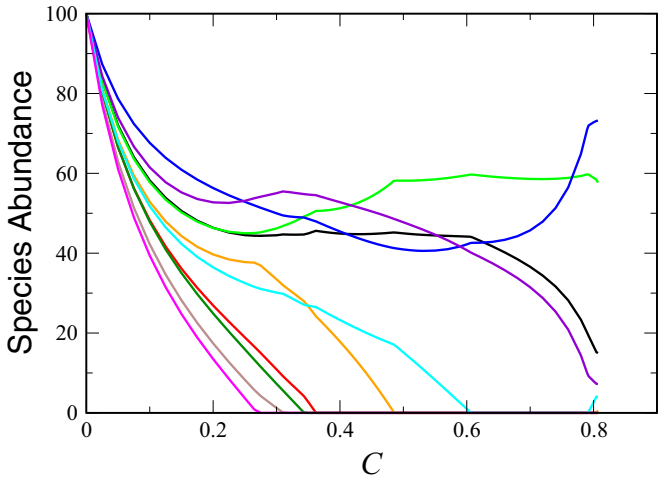

FIG. 4. (Color online) Abundance vs competition. The abundance of $Q = 10$ species on the island is plotted vs the competition parameter C, for a deterministic GCLV model with $K = 100$ and $\sigma = 0.5$, without immigration ($\lambda = 0$). Each color represents the abundance of a different species. In the noninteracting limit $C = 0$ the abundance of all species is identical and equal to K. At $C_1 \approx 0.28$ the abundance of the "weakest" species reaches zero; this is the May transition, where the system enters the competitive exclusion phase. Upon increasing C, more and more species go extinct until (here, around $C = 0.78$) a species comes back to life, as the competitors that suppressed it were themselves suppressed.

VII. MAY TRANSITION AND THE PARTIAL COEXISTENCE PHASE

As C increases even more, the deterministic dynamics (without immigration) no longer supports a steady state with all the Q mainland species coexisting. In the full coexistence phase, as discussed above, the $\lambda = 0$ steady-state system admits a solution [Eq. (6)], which is both feasible ($N_i > 0$) and stable (the real part of all the eigenvalues of the linear stability matrix are negative). As follows from the work of May [30], the chance for the system to fulfill these requisites, for fixed heterogeneity σ, decreases exponentially with Q. In fact, for the GCLV in the coexistence phase, the main obstacle is feasibility [31]. Equation (6) suggests that the solution will be feasible when the sum of all the rows of B^{-1} is positive. As the average sum of a row approaches zero with C, the chance to pick only positive values for N_i decreases exponentially with Q.

In Fig. 4, one observes that for the particular realization of the $c_{i,j}$ being simulated here, with $Q = 10$, the abundance of the weakest species reaches zero around $C = 0.28$. This point marks the transition from the full coexistence phase to the partial coexistence phase. In this phase, the island species richness S is smaller that the mainland richness Q,

as some populations are not supported anymore on the island. Weak competitors (species that suffer from strong competition against others that do not suffer as much) are selected out.

This is the deterministic picture without migration. With migration, "exclusion" does not correspond to exactly zero density. Instead, above the May transition the deterministic density of these species is $\mathcal{O}(\lambda)$. Since we assume that λ is small, demographic noise induces frequent extinction of these transient species. As opposed to the other, "semiresident" species (the "semi" prefix taking account of the possibility of a short-lived absence due to demographic fluctuations), the growth rate of a transient species immigrant is negative, rendering its average persistence times small, independent of K.

Technically speaking, the May transition takes place at a critical value of the competition parameter C_1, where the smallest N_i reaches zero. Above the transition one can define a reduced system, eliminating the row and column of B associated with the eliminated species. This reduced system does admit a solution where all the (remaining) species have positive abundance. This is clear since at the exact value of C at which the next species vanishes, the remaining N_i's constitute a solution of the reduced problem. In addition, the equation for the species with vanishing abundance (call it k) reads as

$$0 = 1 - (C/K)\sum_{j\neq k} c_{k,j}N_j. \tag{8}$$

The right-hand side of this equation is just the growth rate of the kth species, so that for C smaller than the critical value, the growth rate of this species is positive, and for C above this value, it is negative. Thus, the kth species cannot invade for C's slightly larger than the value at which that species disappears from the community.

In Fig. 5, we present the May line in the C-σ plane, showing the dependence of C_1 on σ. The data were obtained by calculating the May point for a set of 100 random $c_{i,j}$ matrices for a given σ and averaging. We see that C_1 increases with decreasing σ, and appears to approach unity for $\sigma \to 0$. We shall return to this point later.

Increasing C in this manner in the partial coexistence phase, one obtains a nested hierarchy of solutions, each with less diversity, which are immune to invasion by any of the extinct species. As mentioned, this hierarchy is completely independent of the carrying capacity K. This prescription eventually breaks down. At some point, there is a "resurrection" of one of the eliminated species. This happens when the species in question was strongly suppressed by another species. As C increases, this suppressor species is itself reduced in abundance, and so the suppressed species is able to stage a comeback. Thus, there is a value of C at which this suppressed species is able to invade. At this point, it needs to be added back to the reduced system since the small external flux will reintroduce it and it will then grow in abundance. Increasing C further, things continue on in this fashion, losing and regaining species. The main characteristic of the partial exclusion phase, the distinction between semiresident species that admit a finite population and $\mathcal{O}(\lambda)$ transients that cannot invade, still holds.

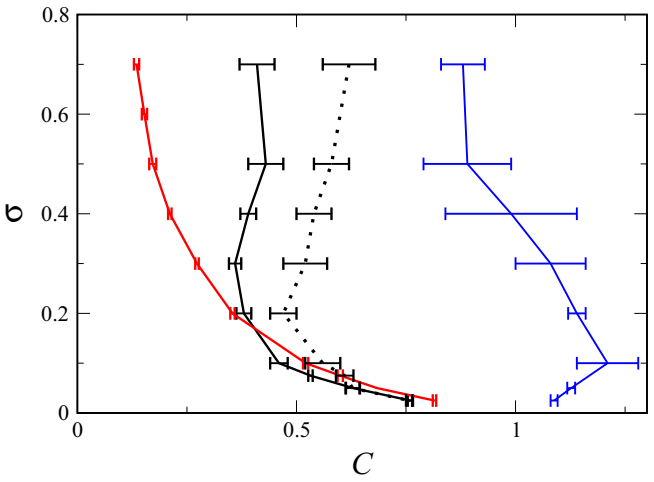

FIG. 5. (Color online) The phase boundaries in the C, σ plane. The leftmost, red, line is the May line where the deterministic solution with all species present disappears. The next, solid black, line to the right is the simulationally determined line where the concave downward part of the species occupancy curve disappears, for the case $K = 100, \lambda = 0.01$. The dotted black line to the right of the solid black line is the same line for $K = 200$, $\lambda = 0.01$. The rightmost, blue, line marks the region where the system spends more than 20% of its time in a particular state, for $K = 100$, $\lambda = 0.01$. The May line was determined by averaging over 100 different realizations of the interaction matrix. The other lines result from averages over 10 or 20 matrices.

An example of the stochastic version of this partial coexistence phase can be seen in the second and third panels of Fig. 2. For this realization of the $c_{i,j}$, with $Q = 20$, the May transition point is at approximately $C_1 \approx 0.169$. We show in Fig. 6 the time-averaged abundances of the species for an extended version of the run presented in the second panel of Fig. 2, with $C = 0.25$, past the May point. We see that

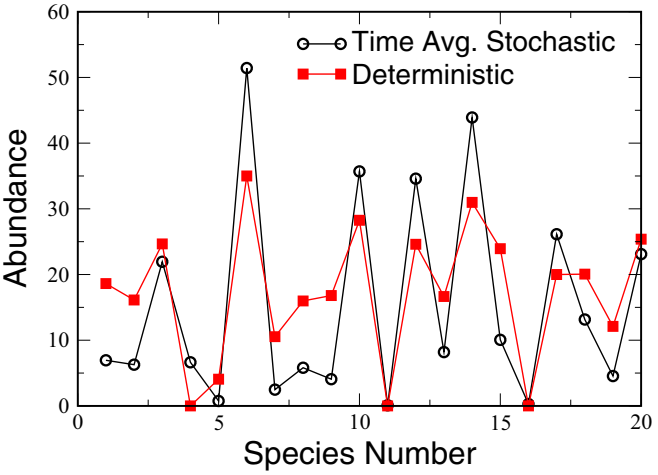

FIG. 6. (Color online) The time-averaged abundance (open circles) vs species number for an extended run of the second panel of Fig. 2. $C = 0.25$, $N = 20$, $K = 100$, $\sigma = 0.5$, $\lambda = 0.01$. Also shown is the deterministic time-independent solution (filled squares). The lines are shown just to guide the eye.

the deterministic solution is essentially missing three species, {4, 11, 16}. The stochastic run shows that the overall structure of the abundance versus species of the deterministic model is preserved. The smaller species are, as might be expected, more severely impacted by the demographic noise, to the benefit of the larger species, which do not have to suffer as much competition from these small species. As C increases, not only does the number of species present in the deterministic solution decrease, but a significant fraction of these have very small abundances. This is reflected in the sharp fall of the IPR in this range of C.

VIII. PHASE III: THE "DISORDERED" PHASE

At some point, C_2, the partial coexistence picture breaks down. In the deterministic model (with immigration), random initial conditions no longer always converge to a fixed steady state, or to any steady state. Typically, slightly beyond C_2 the deterministic system supports a large amplitude periodic attractor. This is demonstrated in Fig. 7, where the percentage of runs that converged to a steady state for a particular $Q = 20$, $\sigma = 0.5$ system is plotted as a function of C. We see that between $C = 0.66$ and 0.67, the percentage of runs that converge to a steady state drops precipitously. This behavior was also seen at a range of different Q's ranging for $Q = 10$ to 100 (data not shown).

The dynamics in the stochastic model in this Phase III diverges significantly from its deterministic counterpart. During the large amplitude deterministic excursions, some species attain low abundance, and are then very vulnerable to extinction. Once extinct, it takes a while for them to return and meanwhile the system falls into a different mode of operation. The system thus irregularly jumps from a set of dominant species to another, in sharp contrast to the deterministic dynamics. An example of this can be seen in Fig. 8, where the deterministic behavior in the left panel stands in sharp contrast to that of the stochastic system with $K = 100$ in the right panel. There is no longer a fixed set of "resident" species which are always present in large numbers. Instead, there is a constant turnover in the set of species present, with the dominant species of the deterministic attractor playing no special role in general. This is reflected in the rise seen in the IPR in Fig. 3 for $C \gtrsim 0.45$.

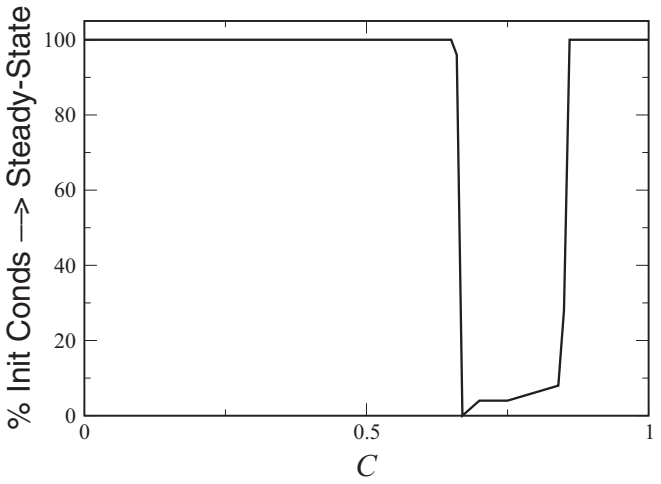

FIG. 7. The percent of runs with random initial conditions that converged to a steady state, as a function of the competition strength C. The matrix $c_{i,j}$ is the same as in Fig. 4, so that $Q = 20$, $\sigma = 0.5$. Also, $\lambda = 0.01$, $K = 100$.

This rise in the IPR occurs significantly before the onset of Phase III in the deterministic model, as the stable state is evidently fragile even before the nontrivial deterministic attractor is born. Thus, as is usual, the sharp transition in the deterministic model is smeared somewhat in the stochastic system. To get a handle on the effective onset of Phase III in the stochastic model, we need to define an "order parameter" to characterize the transition. One such measure is the IPR, which however is computationally expensive to measure accurately.

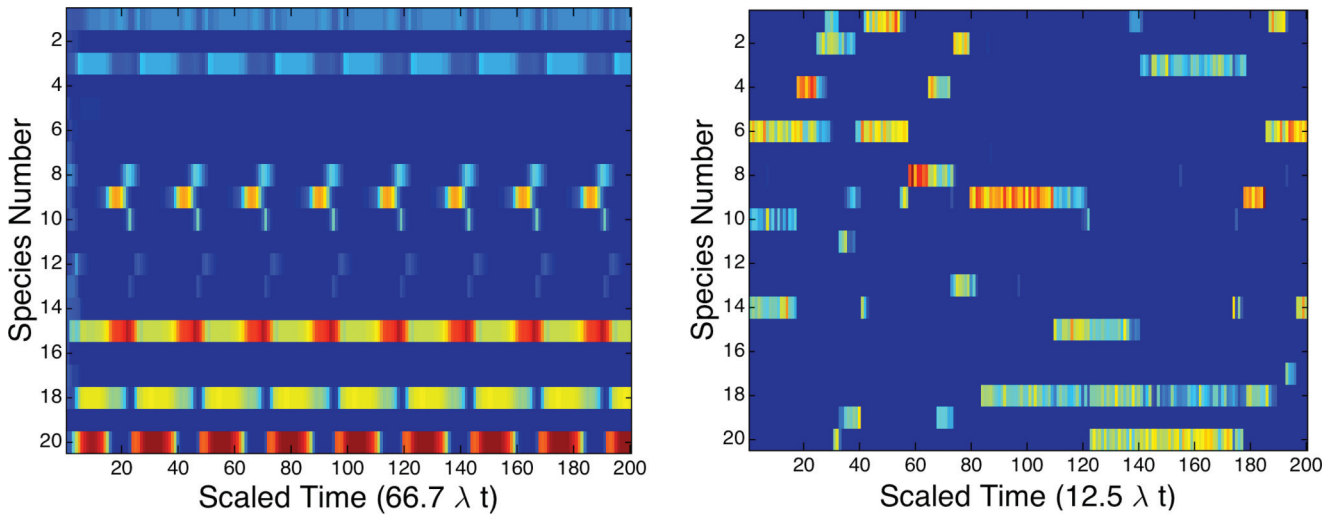

FIG. 8. (Color) Comparison of the time evolution of the deterministic and stochastic dynamics, showing snapshots of the abundance for all species for the two models. Red is high abundance, dark blue low. $Q = 20$, $K = 100$, $C = 0.675$, $\sigma = 0.5$, $\lambda = 0.001$. Left: The deterministic model, with time between snapshots of $\lambda t = 0.015$. Right: The stochastic model, with time between snapshots of $\lambda t = 0.128$. This larger period was chosen in order to exhibit the wide variety of states generated by the stochastic model.

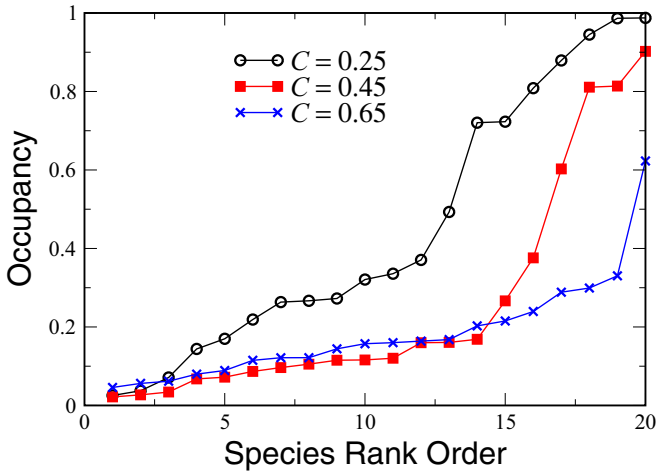

FIG. 9. (Color online) The occupancy vs rank species order (of increasing occupancy) for an extended run of the second, third, and fourth panels of Fig. 2. $C = 0.25$ (open circles), $C = 0.45$ (filled squares), $C = 0.65$ (x's). $Q = 20$, $K = 100$, $\sigma = 0.5$, $\lambda = 0.01$. The lines are shown just to guide the eye.

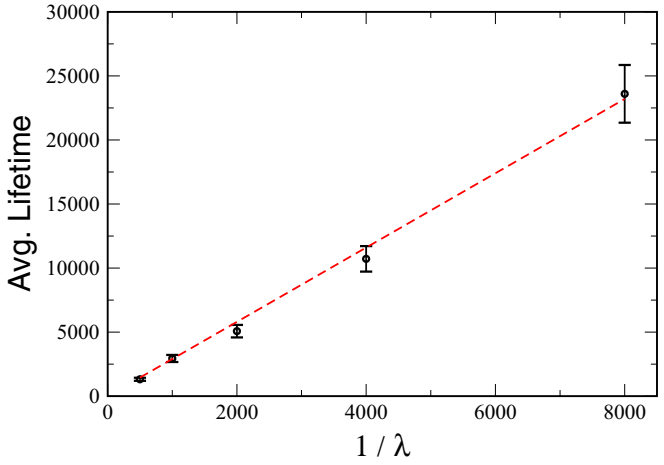

FIG. 10. (Color online) The average dwell time of the invadable state with species {15,18,20} for the $Q = 20$, $C = 0.675$ system simulated in Fig. 4, as a function of $1/\lambda$, showing that the dwell time is inversely proportional to λ. The dotted curve is a straight line to help guide the eye.

Instead we use a measure based on the "occupancy" of each species, the fraction of time that it is present on the island. In Fig. 9, we show the occupancy for the (extensions of the) runs in Fig. 2. We see that for $C = 0.25$, in the partial coexistence phase, there is a set of seven species with relatively high occupancy. These give the overall curve for $C = 0.25$ a concave downward form at high rank order. The number of high occupancy species drops to three at $C = 0.45$, and at $C = 0.65$ the concave downward part of the curve has disappeared and the entire curve is convex upward. Thus, beyond the rise in the IPR, another sign of the end of the partial coexistence phase is the disappearance of the concave downward part of the occupancy curve. We will adopt this as our operational criterion for the location of the phase boundary. In practice, what we do is construct the straight line curve connecting the first and last points of the occupancy curve. If any point in the right half of the occupancy curve lies above this line, the value of C is assigned to the partial coexistence phase. In Fig. 5, we show the phase boundary measured in this manner. We find that the partial coexistence phase becomes narrower as σ decreases, and disappears below some value of σ. In the stochastic model, the transition as measured according to our operational definition clearly depends on the carrying capacity K. Increasing K moves the start of the "disordered" phase to larger C, as can be seen in Fig. 5, consistent with our finding for the deterministic transition point.

As we have mentioned above, the dramatic difference between the deterministic and the stochastic dynamics in this phase has to do with local extinctions. Under demographic noise, a species with a deterministic orbit that takes it close enough to zero abundance may go extinct, and once this happens, it goes out of the game until the next immigrant from this species arrives from the mainland and manages to establish. With small values of λ, this quasistable state persists for relatively long times, many species are absent from the competition so the effective number of species is smaller, and the system can find a steady state, as if it was in the partial coexistence phase.

However, unlike the local minima in a glassy energy landscape, here every local attractor is unstable to invasion by at least one of the Q species on the mainland. The dwell time distribution for an invadable state is exponential, with the mean dwell time inversely proportional to the migration rate λ (at least for not too small K). This relationship is seen clearly in Fig. 10, where the mean dwell time is plotted against $1/\lambda$ for a particular invadable state. Accordingly, the stability of a local attractor is determined by two factors. One is the number of potential invaders, and the other is the low-density growth rate(s) of the invader(s).

This insight suggests the use of a snapshot quenching method to clarify the behavior of the stochastic system. As with a physical system at finite temperature which has a number of metastable states, the momentary state of the system is not at the bottom of a given well, but rather somewhere in its vicinity due to the thermal fluctuations. The way to identify the transitions is to ask, at every instance of time, in which well the system is in. Then, we have a description of the system which is constant as long as the system remains in the well surrounding a given fixed point, and jumps discontinuously when it transitions from one well to another. This description serves to filter out the less interesting small fluctuations within a given well while preserving the major qualitative regime shifts between different wells. One way to determine which well the system is currently in is to quench the system, turning off the thermal fluctuations. We essentially adopt the same procedure here, where instead of potential wells, we have basins of attraction of various steady-states. Taking the state of the stochastic system at a certain time t, we have used it as an initial condition for the deterministic dynamics of Eq. (4) with $\lambda = 0$, and integrate numerically this system until it relaxed to a steady state. (Very rarely, the system relaxes to a more complicated dynamical state, which we characterize by its time-averaged abundances.) This snapshot

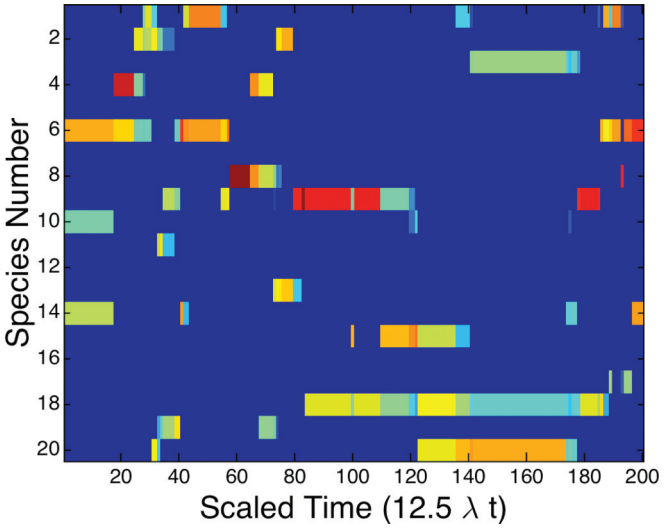

FIG. 11. (Color) Snapshots of the time evolution of the quenched state, i.e., the species abundances of the deterministic $\lambda = 0$ steady-state attractor associated with each of the 200 snapshots in time illustrated in the right panel of Fig. 8.

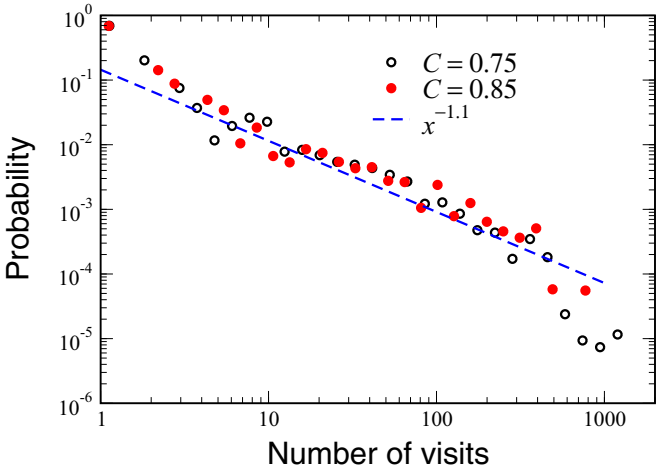

FIG. 12. (Color online) Probability distribution for the number of visits to the various invadable metastable states in a run of total duration $\lambda t = 2 \times 10^4$, with snapshots taken each $\lambda t = 0.08$ for a total of 2.5×10^5 snapshots. Data are shown for $C = 0.75$ and 0.85. For $C = 0.75$, a total of 598 different states were visited, out of a total of 2045 states. $N = 20$, $K = 100$, $\lambda = 0.01$. Also shown is the power law $P(x) \sim x^{1.1}$, which is a good description of the distribution for all but the most visited states.

quenching procedure indicates the species composition of the local attractor at t. Repeating this procedure for every snapshot, taken at intervals of Δt, the quenching produces a description where the system is quiescent for some period of time and then jumps to a new state. These various states are metastable with respect to the species that are present, but typically invadable by species which are currently not represented on the island. Figure 11 shows the results of the quenching procedure for the same stochastic dynamics depicted in the right panel of Fig. 8. We see that it reproduces the species content of the dominant species at each instant of time, but has removed the short-time fluctuations inherent in the stochastic model.

Once successfully invaded, the system leaves the local attractor and wanders around until it finds another local attractor. One may think about the local attractor as an abstract network, where each local attractor is a node and two attractors are connected by a link if the system may jump directly from one of them to the other. This network is seen to have an interesting structure. Figure 12 shows the statistics of number of visits per local attractor, which is very wide and suggests a (cutoff) power law. There are a relatively few number of hub states which are visited in a significant fraction of the transitions, with a large number of states that are visited relatively infrequently. For example, for $C = 0.75$, the most frequently visited state is the invadable state {6, 14}, which was visited 1351 times out of 37 543 transitions. The next most visited states had 1231, 907, and 732 visits, respectively.

It should be emphasized that the topology of this network is much more important, dynamically, than the stability properties of a state. Actually, for $C = 0.75$ there are three stable uninvadable states. The stable state {1,3,15,18,20}, however, was only visited twice, and each time lasted only one snapshot. The other two stable states were not visited at all. Thus, these stable states, for the value of $K = 100$ we are studying, are dynamically irrelevant. We shall return to this point later when we discuss the phase at higher C where various stable states do play a significant role.

The power-law distribution of numbers of visits suggests an interesting transition network, with a very heterogeneous structure. Quantifying the degree distribution of the emerging network we have found that is quite close to be scale free. It shows a power-law decay of the probability of a node to have k links, $P(k)$, with a small exponent (≈ 1.1), in the case demonstrated in Fig. 13, superimposed on a slow exponential cutoff.

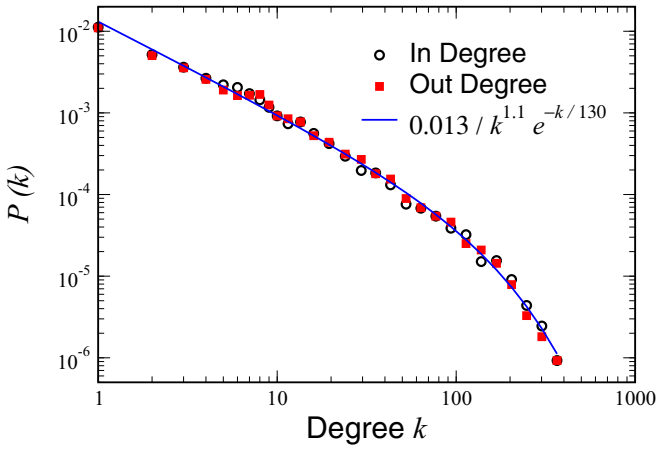

FIG. 13. (Color online) Distribution of the in and out degrees for the transitions between the 3729 states encountered in a long run $N = 40$, $C = 0.4$, $K = 100$, $\lambda = 0.01$.

IX. STRONG COMPETITION AND PHASE IV: THE GLASSLIKE PHASE

We have already mentioned that above C_2, nonstationary attractors can coexist with one or more stable stationary states. However, these stationary states had small basins of attraction in addition to containing species with small abundances. Thus, in the stochastic dynamics they were visited infrequently and had short lifetimes (at least for K's less than 10^4 or so) and so their dynamical relevance was marginal. This situation changes qualitatively beyond some larger value of C, C_3. This can be seen by extending our measurements of the fate of random initial conditions to larger C. We see in Fig. 7 that between $C = 0.84$ and 0.86, the percent of runs that converge to a (one of a number of) steady state rises to 100%. This change in behavior is also readily apparent in the last panel of Fig. 4, and is correlated with the fall of the IPR at large C.

In the stochastic model, the steady states have finite lifetimes, of course. These lifetimes are controlled by K and only weakly impacted by decreasing λ. Due to the small number of species represented in these states, they also are visited relatively frequently. As C increases further, the depth of the various stable solutions increases nonuniformly, and one state eventually dominates. We operationally define the onset of this fourth phase in the stochastic model as the value of C in which the system dwells in a single state for over 20% of the time. The last phase boundary is illustrated in Fig. 5. It should also be noted that as opposed to a true glass, the number of attractors here is not exponentially large. Nevertheless, the dynamics is very slow compared to the disordered Phase III.

X. ENCOUNTER AT THE HUBBELL POINT

As indicated in Fig. 5, the transition lines between the various phases appear to meet at the Hubbell point. Clearly, for any fixed $C < 1$ the deterministic model supports full coexistence when $\sigma \to 0$, implying that the May line must hit the Hubbell point. Similarly, for fixed $C > 1$ and vanishingly small σ every solution with one species of abundance K is uninvadable, so the line separating the "disordered" phase from the glasslike phase also has to reach to the Hubbell point. It is difficult to implement our operational procedures for determining the phase boundaries in the vicinity of the Hubble point, due to the weak stability of the attractive manifolds in this region, which the noise will smear out. However, Fig. 5 indicates the merging of the May line and that separating the partial coexistence and the "chaotic" phases moves to smaller σ for increasing K. If the latter boundary indeed extends down to $\sigma = 0$ for larger enough K, it must also hit the Hubbell point.

The theory of Hubbell, assuming strict neutrality of all species in the community, was criticized for this unrealistic assumption. In particular, it was stressed that any deviation from a strict neutrality must lead to a fixation of the system by the fittest species [32]. As we see here, the situation is more complicated. $C = 1, \sigma = 0$ is apparently a quadracritical point, with slight deviations from perfect neutrality yielding different results, depending on the ratio between C and σ. When superimposed on the effect of noise (and, in particular, of demographic stochasticity that allows for the quasiabsorbing states) the phase diagram may be very rich.

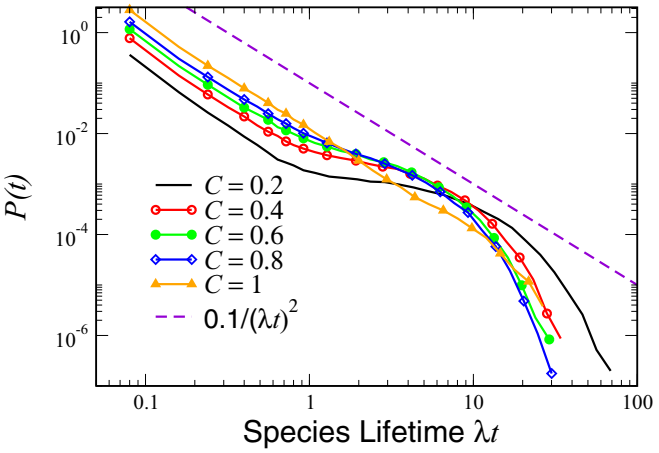

FIG. 14. (Color online) Distribution of species lifetimes, for $Q = 20, \sigma = 0.0156, K = 1000, \lambda = 0.01$ for $C = 0.2$ (black, no marker), 0.4 (red, open circle), 0.6 (green, filled circle), 0.8 (blue, diamond), and 1 (orange, triangle). The (dashed) line $y = 0.1/(\lambda t)^2$ is shown to guide the eye.

One particular example is the distribution of persistence (colonization to extinction) times of species (as opposed to states, which are characterized by a given set of extant species). Figure 14 shows this distribution slightly above the Hubbell point, i.e., for $C = 1, \sigma = 0.0156$. We see that the distribution of species lifetimes is quite wide. Indeed, Fig. 14 suggests a power-law distribution with an exponent close to 2, which resembles the findings of [7].

XI. DISCUSSION AND CONCLUDING REMARKS

The mainland-island system, considered herein, is one of the main models of spatial ecology. It played an important role in the empirical assessment of the two leading pictures of neutral dynamics: the Wilson-MacArthur model (in which all species are equivalent, i.e., admit the same extinction and recolonization rates) and the Hubbell neutral biodiversity model (where all *individuals* are demographically equivalent). In particular, the success of Hubbell in explaining the species abundance distribution in tropical forests, which is the main achievement of the neutral theory of biodiversity, depends entirely on the mainland-island structure, since the species abundance distribution of a simple well-mixed model does not fit the empirical data.

In light of this, the rich structure of the mainland-island competitive Lotka-Volterra system that revealed itself in this study appears to be very interesting. Clearly, the perfect neutrality of Wilson-MacArthur and Hubbell models depends on unrealistic fine tuning of the system parameters, so one would like to figure out what happens when this assumption is relaxed. It turns out that the answer to this question is quite subtle, in particular close to the Hubbell point. Slight deviations from the perfectly neutral scenario may lead to absolutely different dynamical behaviors, and the role of noise close to the transition is crucial.

Our work opens up a few interesting questions about the dynamics of local and global communities. First, one would like to characterize the dynamics of empirical communities

as belonging to one of the four qualitative phases considered above. With databases such as the North-American Breeding Birds survey, giving the yearly community composition in thousands of locations along about 45 years, this task may be achievable. Once the dynamics of a local community is understood, the overall species turnover rates in a system of local patches connected by migration (a metapopulation) may be investigated both theoretically and by an analysis of field data. One possibility that emerges from our study is that, in such a metacommunity of disordered or glassy patches, the time to extinction of an extinction-prone species will be so large that it will reach the evolutionary scale (the speciation time) and thus the biodiversity puzzle will be solved.

Two technical points also merit some discussion. First, although the noise introduced into the model is purely demographic, i.e., it scales with the square root of the population size, the abundance fluctuations are much larger, as clearly seen in Fig. 2. The reason is that the demographic noise is superimposed on the nonlinear effects of the deterministic dynamics. This phenomenon is in agreement with many recent studies [33–35], showing that the noise in empirical systems is clearly stronger than demographic. Moreover, at least for large K one should expect that the large abundance semiresident species are less affected by the noise than the rare species, such that the scaling of abundance fluctuations with N_i will be stronger than the square root of N_i but weaker than N_i; this is indeed the case in some empirical systems [33].

A second issue, somehow connected to the first, is the effect of "real" environmental noise, i.e., time dependent fluctuations of the model parameters. Environmental stochasticity is usually considered as a destabilizing factor, increasing species turnover rate and the amplitude of abundance fluctuations, but it may also stabilize a $c_{i,j}$ independent equal abundance fixed point due to the storage effect [36]. We hope to address this issue in a subsequent publication.

Finally, we believe that the classification presented here, although only semiqualitative at present, is very important to the understanding of community dynamics in general. In most cases, the data analyzed by researchers reflect the local species richness rather than the state of a regional pool, but is interpreted as a fairly honest sample of the global community, assuming, more or less, that the system is either in the full coexistence or in the partial coexistence phase. Such an interpretation may be misleading. In particular, in the disordered and in the glassy phase, sudden drastic variations in the structure of the community reflect the intrinsic dynamics of the system and, in contrast to a very common interpretation, are not evidence for exogenous factors that induce a catastrophic shift. As the concerns about the impact of anthropogenic changes rise, it is imperative to take this possibility into account.

ACKNOWLEDGMENT

This work was supported by the Israeli Ministry of Science TASHTIOT program and by the Israeli Science Foundation BIKURA Grant No. 1026/11 (N.M.S.) and by the Israel Science Foundation Grant No. 376/12 (D.A.K.).

[1] G. Hardin, Science **131**, 1292 (1960).
[2] E. Pennisi, Science **309**, 90 (2005).
[3] R. O. Bierregaard, Ecology **91**, 2806 (2010).
[4] L. S. Tsimring, Rep. Prog. Phys. **77**, 026601 (2014).
[5] R. Lande, S. Engen, and B.-E. Saether, *Stochastic Population Dynamics in Ecology and Conservation* (Oxford University Press, Oxford, UK, 2003).
[6] P. Chesson, Annu. Rev. Ecol. Syst. **31**, 343 (2000).
[7] E. Bertuzzo, S. Suweis, L. Mari, A. Maritan, I. Rodríguez-Iturbe, and A. Rinaldo, Proc. Natl. Acad. Sci. USA **108**, 4346 (2011).
[8] O. Allouche and R. Kadmon, Ecol. Lett. **12**, 1287 (2009).
[9] D. Gravel, C. D. Canham, M. Beaudet, and C. Messier, Ecol. Lett. **9**, 399 (2006).
[10] R. A. Chisholm and S. W. Pacala, Proc. Natl. Acad. Sci. USA **107**, 15821 (2010).
[11] T. Zillio and R. Condit, Oikos **116**, 931 (2007).
[12] D. Tilman, Am. Nat. **129**, 769 (1987).
[13] S. Pigolotti, C. López, and E. Hernández-García, Phys. Rev. Lett. **98**, 258101 (2007).
[14] H. Fort, Entropy **15**, 5237 (2013).
[15] R. H. MacArthur, *The Theory of Island Biogeography* (Princeton University Press, Princeton, NJ, 1967), Vol. 1.
[16] J. B. Losos and R. E. Ricklefs, *The Theory of Island Biogeography Revisited* (Princeton University Press, Princeton, NJ, 2009).
[17] S. P. Hubbell, *The Unified Neutral Theory of Biodiversity and Biogeography* (Princeton University Press, Princeton, NJ, 2001).
[18] J. Rosindell, S. P. Hubbell, and R. S. Etienne, Trends Ecol. Evol. **26**, 340 (2011).
[19] C. K. Fisher and P. Mehta, Proc. Natl. Acad. Sci. USA **111**, 13111 (2014).
[20] S. Pigolotti and M. Cencini, J. Theor. Biol. **338**, 1 (2013).
[21] G. Bell, Am. Nat. **155**, 606 (2000).
[22] D. A. Kessler, J. Appl. Probab. **45**, 757 (2008).
[23] Y. Ben-Zion and N. M. Shnerb, Oikos **121**, 985 (2012).
[24] S. Suweis, E. Bertuzzo, L. Mari, I. Rodriguez-Iturbe, A. Maritan, and A. Rinaldo, J. Theor. Biol. **303**, 15 (2012).
[25] D. A. Kessler and N. M. Shnerb, J. Stat. Phys. **127**, 861 (2007).
[26] I. Volkov, J. R. Banavar, S. P. Hubbell, and A. Maritan, Nature (London) **424**, 1035 (2003).
[27] O. Malcai, O. Biham, P. Richmond, and S. Solomon, Phys. Rev. E **66**, 031102 (2002).
[28] D. A. Kessler and N. M. Shnerb, J. Theor. Biol. **345**, 1 (2014).
[29] E. Seri, Y. E. Maruvka, and N. M. Shnerb, Am. Nat. **180**, E161 (2012).
[30] R. M. May, Nature (London) **238**, 413 (1972).
[31] I. D. Rozdilsky and L. Stone, Ecol. Lett. **4**, 397 (2001).
[32] S.-R. Zhou and D.-Y. Zhang, Ecology **89**, 248 (2008).
[33] M. Kalyuzhny, Y. Schreiber, R. Chocron, C. H. Flather, R. Kadmon, D. A. Kessler, and N. M. Shnerb, Ecology **95**, 1701 (2014).
[34] R. A. Chisholm, R. Condit, K. A. Rahman, P. J. Baker, S. Bunyavejchewin, Y.-Y. Chen, G. Chuyong, H. Dattaraja, S. Davies, C. E. Ewango *et al.*, Ecol. Lett. **17**, 855 (2014).
[35] M. Kalyuzhny, E. Seri, R. Chocron, C. H. Flather, R. Kadmon, and N. M. Shnerb, Am. Nat. **184**, 439 (2014).
[36] P. Chesson, Theor. Population Biol. **45**, 227 (1994).